HHS Public Access

Author manuscript

Nature. Author manuscript; available in PMC 2012 June 01.

Published in final edited form as:

Nature. ; 480(7375): 109–112. doi:10.1038/nature10632.

Lyn is a redox sensor that mediates leukocyte wound attraction in vivo

Sa Kan Yoo[1], **Taylor W. Starnes**[2], **Qing Deng**[2], and **Anna Huttenlocher**[2,3,*]

[1]Program in Cellular and Molecular Biology, University of Wisconsin-Madison, Madison, WI 53706, USA

[2]Department of Medical Microbiology and Immunology, University of Wisconsin-Madison, Madison, WI 53706, USA

[3]Department of Pediatrics, University of Wisconsin-Madison, Madison, WI 53706, USA

Summary

Tissue wounding induces the rapid recruitment of leukocytes[1]. Wounds and tumors, a type of "unhealed wound"[2], generate hydrogen peroxide (H_2O_2) through a NADPH oxidase (NOX) and the extracellular H_2O_2 mediates recruitment of leukocytes, particularly first responders of innate immunity, neutrophils, to injured tissue[3–6]. However, it is not known what sensor neutrophils use to detect the redox state at wounds. Here we identify the Src family kinase (SFK) Lyn as a redox sensor that mediates initial neutrophil recruitment to wounds in zebrafish larvae. Lyn activation in neutrophils is dependent on wound-derived H_2O_2 following tissue injury and inhibition of Lyn attenuates neutrophil wound recruitment. Inhibition of SFKs also disrupted H_2O_2-mediated chemotaxis of primary human neutrophils. In vitro analysis identified a single cysteine residue, C466, as being responsible for direct oxidation-mediated activation of Lyn. Furthermore, transgenic tissue-specific reconstitution with wild-type Lyn and a cysteine mutant revealed that Lyn C466 is important for the neutrophil wound response and downstream signaling in vivo. This is the first identification, to our knowledge, of a physiological redox sensor that mediates leukocyte wound attraction in multicellular organisms.

Paracrine signaling by hydrogen peroxide (H_2O_2) induces neutrophil wound attraction[6]. However, it is not known what sensor detects H_2O_2 and mediates neutrophil recruitment. H_2O_2 can cross cell membranes and inactivate tyrosine phosphatases through oxidation of the catalytic cysteine[7–11]. Cysteine oxidation also regulates protein kinases[12–15]. We used

*Corresponding author. Mailing address: Anna Huttenlocher, 4205 Microbial Sciences Building, 1550 Linden Dr., Madison, WI 53706; Phone: (608) 265–4642; FAX: (608) 262–8418. huttenlocher@wisc.edu.

Supplementary Information

There are 13 supplementary figures and 4 movies.

Author Contribution

S.Y. designed the research, performed the experiments, analyzed data and wrote the paper. T.W.S. contributed to development and data analysis of in vitro chemotaxis assay. Q.D. constructed HyPer probe and contributed expertise in zebrafish injection. A.H. designed the research, analyzed data and co-wrote the paper.

The authors declare no competing financial interests.

zebrafish, which are a powerful system to study vertebrate immunity[6, 16–19], to identify a mechanism by which neutrophils detect wound-induced H_2O_2. While searching for a neutrophil redox sensor, we found that Src family kinases (SFKs) are activated in neutrophils around wounds. We detected autophosphorylation of the activation loop tyrosine of SFKs at 30 minutes post tail transection in 3 days-post-fertilization (dpf) larvae (Fig. 1a,b,c). Phosphorylated SFKs displayed a punctate appearance at the neutrophil leading edge and the autophosphorylation depended on wounding (Fig. 1b,c, Supplementary Fig. 2a,b). SFKs maintain inhibitory intramolecular interactions in an inactive state, while dephosphorylation of the C-terminal phosphotyrosine releases the inhibitory configuration, allowing trans-autophosphorylation of the activation loop tyrosine, thereby activating SFKs[20–23]. Additionally, emerging evidence suggests cysteine redox-mediated regulation of SFKs[13, 15]. Several cysteines are implicated in the redox regulation of cSrc[13, 15], but redox regulation of other SFKs is poorly understood.

To investigate whether H_2O_2 is involved in SFK autophosphorylation in neutrophils, we inhibited NADPH oxidase (NOX) enzymes with diphenyleneiodonium (DPI)[6]. DPI attenuated SFK phosphorylation in neutrophils after wounding (Supplementary Fig. 2c,d). To distinguish H_2O_2 production from neutrophils versus wounds, we used morpholino antisense oligonucleotides to interfere with pre-mRNA splicing of dual oxidase (duox), which is responsible for H_2O_2 generation at wounds, but not in neutrophils[6]. Duox knockdown inhibited SKF phosphorylation in neutrophils (Fig. 1d,e), indicating that SFK phosphorylation depends on the H_2O_2 burst at wounds.

We found that treatment with SFK inhibitors impaired early accumulation of neutrophils at wounds (Fig. 1f,g, Supplementary Fig. 2e,f and Supplementary Fig. 3a,b). We focused on early recruitment of neutrophils to wounds at 0.5–1h post wounding throughout this study, because within this time frame the H_2O_2 burst occurs[6] (Supplementary Movie 1) and neutrophil accumulation is roughly linear[18, 19]. Addition of PP2 at 1h post wounding did not disturb resolution of inflammation, which is mediated by neutrophil reverse migration from wounds[16, 19] (Supplementary Fig 3c.d). SFK inhibition did not impair H_2O_2 burst at wounds (Fig. 1h and Supplementary Movie 1) or neutrophil motility in the cephalic mesenchyme[18] (Supplementary Fig. 2g,h and Movie 2). Injection of H_2O_2 into the otic cavity, or bath application of H_2O_2 following wounding recruited neutrophils, which was impaired by SFK inhibition (Supplementary Fig. 4a,b,c,d,e,f). We also performed an in vitro chemotaxis assay using human neutrophils. Consistent with mouse neutrophils[3], H_2O_2 directly attracted human neutrophils (Fig. 1i). Two structurally different SFK inhibitors impaired chemotaxis to H_2O_2 (Fig. 1i) while SFK inhibition enhanced chemotaxis to fMLP (Supplementary Fig. 4g).

To identify specific SFKs that mediate neutrophil wound responses, we purified zebrafish myeloid cells by fluorescence-activated cell sorting and performed reverse transcription polymerase chain reaction (RT-PCR)[19] (Supplementary Fig. 5a). Among the nine SFKs in mammals, Lyn, Fgr and Hck are myeloid specific[20,24]. Analysis of EST profiles in UniGene (NCBI) suggested that Lyn, Hck, Yrk and Src might be expressed in zebrafish leukocytes. RT-PCR detected lyn in neutrophils and lyn and yrk in macrophages (Fig. 2a). In situ hybridization detected lyn mRNA in the caudal hematopoietic tissue (CHT) as well as in the

pronephric ducts and neuromasts (Fig. 2b). Lyn, which is phylogenetically conserved (Supplementary Fig. 5b), is expressed in all leukocytes except T lymphocytes in mammals, and its deficiency in mice leads to myeloproliferation and autoimmunity[24–26]. Lyn-deficient neutrophils display an exaggerated response to adhesion signals and weakened response to several chemokines in vitro, but its role in neutrophils in vivo is not clear[24, 27]. To knockdown zebrafish Lyn, we designed two morpholinos to target pre-mRNA splice sites (Fig. 2c). Both morpholinos attenuated neutrophil accumulation at wounds (Fig. 2d). Lyn knockdown increased the number of total neutrophils in the CHT (Supplementary Fig 5c,d), consistent with the myeloproliferation of lyn-deficient mice[24–26]. Live imaging demonstrated that Lyn depletion impaired neutrophil directional migration towards wounds (Fig. 2 e,f,g and Supplementary Movie 3). Macrophage wound attraction was inhibited by PP2 or DPI but not Lyn knockdown (Supplementary Fig. 6a,b). Lyn knockdown also inhibited neutrophil responses to bath H_2O_2 (Supplementary Fig. 7a,b). To investigate specificity, we used LTB_4, which attracts zebrafish neutrophils[17]. Bath LTB_4 induced dissemination of neutrophils into fins, which was not prevented by either DPI or Lyn knockdown (Supplementary Fig. 7c,d,e,f and Supplementary Movie 4). Lyn depletion also inhibited the wound-induced SFK autophosphorylation in neutrophils (Fig. 2h,i), indicating that Lyn is primarily responsible for SFK phosphorylation in neutrophils.

We hypothesized that Lyn might be a neutrophil redox sensor that detects H_2O_2 at wounds. When we expressed Lyn fused to GFP at its C-terminus in HEK293 cells, which produce H_2O_2 via NOX4[28], phosphorylation of Lyn activation loop tyrosine was detected (Fig. 3a). This autophosphorylation of Lyn partly depended on endogenous reactive oxygen species (ROS), because NOX inhibition by DPI decreased Lyn phosphorylation (Fig. 3a,b). Because endogenous ROS could also work on phosphatases and other kinases, we took a Lyn-specific approach. We created two cysteine mutants C224A and C466A, mutating each cysteine to alanine, based on the importance of the corresponding residues in cSrc[13] and phylogenetic conservation. When expressed in HEK293 cells, C466A had impaired autophosphorylation while C224A was phosphorylated similarly to Lyn WT (Fig. 3c,d). Cysteine 466 (C466) is located at the C-terminus of the kinase domain and is phylogenetically conserved (Supplementary Fig. 8a). To investigate whether H_2O_2 activates Lyn directly through C466 oxidation, we performed an in vitro kinase assay. After immunoprecipitation of Lyn, we added 15 μM H_2O_2, which is consistent with concentrations that attract neutrophils in vitro[3] (Fig. 1i) and in vivo[6]. H_2O_2 directly activated Lyn WT but not C466A (Fig. 3e,f). Importantly, C466A was activated by magnesium, which is necessary for the kinase reaction with ATP, similarly to WT (Fig. 3g,h), suggesting that C466 regulates the redox-specific function of Lyn rather than the basal activity. We also detected reduced cysteines in Lyn by biotinylated iodoacetamide (BIAM) labeling[13] and found that the C466A was slightly but significantly more reduced than WT (Supplementary Fig. 8b,c), which is consistent with the idea that Lyn has multiple cysteines which could be oxidized. Because mitogen-activated protein kinases (MAPKs) are activated downstream of ROS and SFKs[29], we investigated the effects of Lyn expression on MAPKs. Ectopic expression of Lyn in HEK293 cells, where Lyn is activated by endogenous ROS (Fig. 3a,b), activated Erk but not JNK or p38 (Supplementary Fig. 8d). This Lyn-induced activation of Erk was attenuated in cells expressing Lyn C466A compared to Lyn WT

(Supplementary Fig. 8e,f). Collectively, our data indicate that H_2O_2 directly activates Lyn through oxidation of C466, which activates downstream signaling. We also found that C468 in human Lyn, which corresponds to C466 of zebrafish Lyn, has similar functions in regulating Lyn autophosphorylation and oxidation and Erk activation (Supplementary Fig. 9a,b,c,d,e).

To investigate the importance of Lyn C466 during neutrophil wound responses, we established two transgenic zebrafish lines, which express Lyn WT-GFP and C466A-GFP at similar levels in neutrophils (Supplementary Fig. 10a,b,c,d). We injected lyn morpholino, which does not inhibit the transgenes, into these transgenic animals. Lyn morpholino did not inhibit neutrophil accumulation at wounds in transgenic larvae expressing Lyn WT in neutrophils, although it impaired neutrophil recruitment in wild-type clutchmates (Fig. 4a,b), indicating that Lyn regulates neutrophil wound responses cell-autonomously. When we injected lyn morpholino in the transgenic line expressing Lyn C466A in neutrophils, Lyn knockdown inhibited neutrophil wound responses in the transgenic larvae (Fig. 4c,d). These data demonstrate that C466, which is necessary for H_2O_2-induced Lyn activation, mediates neutrophil responses in vivo. We also investigated the importance of the cysteine to signaling downstream of Lyn in neutrophils in vivo. Erk phosphorylation was detected in puncta at the leading edge of neutrophils around wounds (Supplementary Fig. 11a), which is reminiscent of phosphorylated SFKs (Fig. 1b). Lyn knockdown impaired Erk activation in neutrophils (Supplementary Fig. 11b,c), which was reversed by transgenic expression of Lyn WT in neutrophils but not the C466A mutant, supporting the importance of C466 in vivo (Supplementary Fig. 11d,e,f,g). Furthermore, Erk inhibition impaired neutrophil wound attraction (Supplementary Fig. 12).

In conclusion, we have found, for the first time, that Lyn acts as a direct redox sensor that mediates neutrophil wound responses in vivo (Supplementary Fig. 1a). Oxidation of cSrc regulates its activity, but whether it leads to inhibition or activation has been controversial[13, 15]. Oxidative stress activates Lyn in neutrophils, but whether activation is direct or indirect was not known[30]. Here we have shown that Lyn is activated through direct oxidation of C466 and provide in vivo relevance. Because we did not detect oligomerization of Lyn in non-reducing SDS-PAGE (data not shown), oxidation at C466 might regulate an intramolecular conformation. H_2O_2 can cross the plasma membrane through aquaporins[8, 11]. How redox sensing by Lyn is transformed into directional migration remains to be determined. Activation of Lyn and Erk at the neutrophil front suggests that Lyn might regulate the neutrophil leading edge. Lyn is unique for its dual roles in regulating both inhibitory signaling by phosphatases such as SHIP and activating signaling by MAPKs[24–26] (Supplementary Fig. 1b). How the opposing positive and negative signaling is coordinated is poorly understood. Because the phosphatases comprising Lyn's inhibitory pathway are inactivated by oxidation[9,10], we speculate that H_2O_2 may have two effects on Lyn's function to orchestrate neutrophil wound responses: oxidation-mediated activation of Lyn and inhibition of the redox-sensitive inhibitory signaling downstream of Lyn (Supplementary Fig. 1b).

Methods Summary

Adult AB zebrafish and larvae were maintained as described previously[18]. For live imaging or wounding assay, larvae were anesthetized in E3 containing 0.2 mg/mL Tricaine. To prevent pigment formation, some larvae were maintained in E3 containing 0.2 mM N-phenylthiourea. For morphoino experiments, 2.5–3 dpf larvae were used. For experiments without morpholinos, 3–3.5 dpf larvae were used. Confocal immunofluorescence images were acquired with a confocal microscope (FluoView FV1000, Olympus) using a NA 0.75/20x objective or a NA 1.45/60x oil immersion objective lens. Morpholino oligonucleotides (Gene Tools) in Danieau buffer were injected into 1-cell-stage embryos. Duox splice morpholino (100μM) was injected with p53 morpholino (300 μM) as previously described[6]. Lyn splice morpholino lyn MO1 (5′-TCAGACAGCAAATAGTAATCACCTT-3′) (500 μM) or lyn splice morpholino lyn MO2 (5′-GAGTCTGTATTTCAGTACCATTAGC-3′) (500 μM) was used (Danieau buffer as a control). To generate transgenic lines, 1 nL of solution containing 12.5 ng/μL DNA plasmid (tol2-mpx-lyn-GFP or tol2-mpx-lyn C466A-GFP) and 17.5 ng/μL transposase mRNA was injected into the cytoplasm of one-cell stage embryos. Injected embryos were raised to sexual maturity and screened by crossing with wild-type fish to identify founders. F1 embyros were identified by GFP expression and raised to sexual maturity. Experiments were performed on progeny of F1 or F2 outcross with wild-type fish. HEK293 cells were cultured in DME containing 10% FCS. Cells were transfected using Lipofectamine 2000 (Invitrogen).

Full methods

Zebrafish maintenance and general procedures

Adult AB zebrafish and larvae were maintained as described previously[18]. For live imaging or wounding assay, larvae were anesthetized in E3 containing 0.2 mg/mL Tricaine (ethyl 3-aminobenzoate, Sigma Aldrich). To prevent pigment formation, some larvae were maintained in E3 containing 0.2 mM N-phenylthiourea (PTU, Sigma Aldrich). For morphoino experiments, 2.5–3 dpf larvae were used. For experiments without morpholinos, 3–3.5 dpf larvae were used. When drugs were used, larvae were pretreated at least for 1h before experiments unless otherwise indicated (10–20 μM PP2, 10 μM PP1, 50–100 μM DPI, 100 μM PD98059, 20 μM U0126). Tail transection was performed on 2.5–3 dpf larvae using a razor blade. Tail fins of 3–3.5 dpf larvae were wounded with a needle. For application of exogenous H_2O_2, we injected one nl of 10 μM H_2O_2 into the otic cavity of 3 dpf larvae or bathed 2.5–3 dpf larvae in E3 containing 100 μM H_2O_2 following tail transection. For bath application of LTB_4, 2.5–3 dpf larvae were bathed in E3 containing 30 μM LTB_4.

Immunofluorescence and Sudan Black staining

Thirty minutes after tail transection, 2.5–3 dpf larvae were fixed with 1.5% formaldehyde in 0.1 M PIPES, 1.0 mM $MgSO_4$ and 2 mM EGTA overnight at 4°C and immunolabeled as previously described[19]. We used the following primary antibodies: rabbit anti-MPX antibody[19, 31] at 1:300, rabbit anti-L-Plastin antibody[19, 31] at 1:300, rabbit anti-phospho-Src

family (Tyr416) antibody (Cell Signaling, #2101) at 1:300, rabbit anti-phospho-Src family (Tyr416) antibody (Cell Signaling, D49G4) at 1:300, mouse anti-phospho-Erk1/2 (T185, Y187, T202, Y204) antibody (Abcam, ab50011) at 1:300. For pSFKs staining, the rabbit anti-phospho-Src family (Tyr416) antibody (Cell Signaling, #2101) was used except Supplementary Fig. 2a, which was stained with the rabbit anti-phospho-Src family (Tyr416) antibody (Cell Signaling, D49G4). DyLight 488-or 549-conjugated IgG antibodies (Jackson ImmunoResearch) were used as secondary antibodies. Sudan Black staining was performed as previously described[18, 19].

FACS and RT-PCR

Dissociated cells of *Tg(mpx:Dendra2)* at 3 dpf were sorted by FACS as previously described[19]. RNA was isolated using the RNeasy Mini Kit (Qiagen) and one-step RT-PCR (Qiagen) was performed. Primers for c-fms, mpx and ef1α have been previously described[31]. Other oligo sequences were as follows:

hck forward, 5′-TGCCAGTCTCTCACCTCTCC-3′

hck reverse, 5′-GCCGAAAGACCACACATCGG-3′

lyn forward, 5′-CGAAAGCTGGATAAAGCATGCG-3′

lyn reverse, 5′-CTGCTCTCAGGTCTCGGTGG-3′

yrk forward, 5′-CAGATCATGAAGAGGCTCCGTC-3′

yrk reverse, 5′-CCTGCTCCAGCACCTCTCGG-3′

src forward, 5′-ACGGCCTGTGCCACTCCCTG-3′

src reverse, 5′-CCGTACAGAGCTGCCTCCGG-3′

Morpholino injection and RT-PCR

Morpholino oligonucleotides (Gene Tools) in Danieau buffer (58 mM NaCl, 0.7 mM KCl, 0.4 mM MgSO4, 0.6 mM Ca(NO3)2, 5.0 mM HEPES pH 7.1–7.3) were injected (1 nL) into 1-cell-stage embryos. Duox splice morpholino (5′-AGTGAATTAGAGAAATGCACCTTTT-3′) (100μM) was injected with p53 morpholino (5′-GCGCCATTGCTTTGCAAGAATTG-3′) (300 μM) as previously described (p53 morpholino (300 μM) was used as a control)[6]. Lyn splice morpholino lyn MO1 (5′-TCAGACAGCAAATAGTAATCACCTT-3′) (500 μM) or lyn splice morpholino lyn MO2 (5′-GAGTCTGTATTTCAGTACCATTAGC-3′) (500μM) was used (Danieau buffer as a control). For morphotyping of the splicing morpholinos, RNA was prepared from 2.5–3 dpf larvae using TRIzol (Invitrogen) and one-step RT-PCR (Qiagen) was performed. Primers for duox have been described previously[6]. Other oligo sequences were as follows:

lyn forward (for lyn MO1), 5′-GCGAGGTCTTTGACCACACG-3′

lyn reverse (for lyn MO1), 5′-CGCATGCTTTATCCAGCTTTCGAC-3′

lyn forward (for lyn MO2), 5′-CGAAAGCTGGATAAAGCATGCG-3′

lyn reverse (for lyn MO2), 5′-CTGCTCTCAGGTCTCGGTGG-3′

Whole-mount in situ hybridization

For in situ hybridization, 1 kb of zebrafish lyn C-terminus was amplified with the T7 promoter by RT-PCR (5′-CGTAGACGCTCAGGGCCAGG-3′ and 5′-GATCACTAATACGACTCACTATAGGGTCATGGCTGCTGCTGGTACTGG-3′) using mRNA from 3dpf larvae as a template. Digoxigenin-labeled RNA probe was transcribed with the use of T7 RNA polymerase (Ambion). The mpx probe was transcribed as previously descrbed[32]. 3 dpf larvae were fixed in 4% paraformaldehyde in PBS and mRNA was labeled by in situ hybridization using the previously described protocol[33].

Image acquisition and analysis

Confocal immunofluorescence images were acquired with a confocal microscope (FluoView FV1000, Olympus) using a NA 0.75/20x objective or a NA 1.45/60x oil immersion objective lens. Z-series were acquired using 260–600 μm pinhole. For quantification of fluorescence intensity of pSFK and pErk in neutrophils, the median intensity of a square with three-pixel sides was measured at a single z-plane and the highest median intensity within each neutrophil was utilized. For H_2O_2 imaging, HyPer fluorescence was excited with 405 nm and 488 nm lasers, and emission wavelengths 505–510 and 510–525 nm (dichroic mirror: SDM510, band pass filter: BA505–525) were acquired using the sequential line scanning. Ratiometric analysis was performed by using FluoView FV1000 software (Olympus) after Z-series stacking as previously described[18]. Neutrophils were tracked and analyzed by using plugins MTrackj (3D tracking), Manual tracking (2D tracking) and Chemotaxis and Migration tool (ibidi) for ImageJ (NIH, Bethesda, MD). The percentage of neutrophils that accumulate at wounds was calculated by dividing the number of neutrophils that arrived at a wound during 30 minutes post wounding by the total number of neutrophils in a region that is 400–500 μm distant from the wound margin. A Nikon SMZ-1500 stereomicroscope (Nikon) was used for imaging of larvae labeled with Sudan Black staining and in situ hybridization and time-lapse analysis of *Tg(mpx:Dendra2)*.

Photolabeleing of neutrophils

Neutrophils at wounds were photolabeled as previously described[19]. *Tg(mpx:Dendra2)* at 3dpf were wounded with a razor blade. At one hour after wounding, larvae were treated with DMSO or PP2 and neutrophils at wounds were were photolabeled by photoconverting fluorescence of Dendra2 from green (488 nm) to red (543). For photoconversion, a 405 nm laser was focused into an area of interest for 20–30 s with 20–30% power 10.0 μ/pixel (tornado function). Photolabeled neutrophils were tracked up to 9.5h post wounding

Plasmid construction and in vitro transcription

The plasmid for zebrafish lyn WT expression in HEK293 cells was constructed by subcloning codon-optimized lyn WT (Supplementary Fig. 12a) into pEGFP-N1 vector (clontech). Humanization and optimization of codon usage was performed (GenScript) due to poor expression of original zebrafish lyn in HEK293 cells. Lyn mutants (C466A, C224A and Y506F) in pEGFP-N1 were made by overlap PCR mutagenesis. Codon optimized lyn WT-GFP or C466A-GFP was subcloned into the backbone vector with the mpx promoter[16], minimal tol2 elements[34] and a SV40 polyadenylation sequence as previously described[18, 19].

HyPer[35] was subcloned into the pCS2+ vector, linearized by Not1 and in vitro transcribed by SP6 RNA polymerase (Invitrogen). The plasmid for human lyn WT expression in HEK293 cells was constructed by subcloning codon-optimized human lyn WT (Supplementary Fig. 12b) into pEGFP-N1 vector (clontech). Human lyn C468A in pEGFP-N1 was made by overlap PCR mutagenesis.

Cells and transfection

HEK293 cells were cultured in DME containing 10% FCS. Cells were transfected using Lipofectamine 2000 (Invitrogen) according to the manufacturer's instruction. Cells were treated with DPI for 6–7 hours before lysis in Figure 3a.

Immunoblot analysis

HEK293 cells were lysed in lysis buffer (50 mM HEPES, pH 7.4, 150 mM NaCl, 0.5% Nonidet P-40, 5% glycerol, 1 mM $MgCl_2$, 1 mM $MnCl_2$, 20 mM NaF, 1 mM Na_3VO_4, 1 mM dithiothreitol, 0.2 mM PMSF, 1 μg/ml pepstatin, 10 μg/mlaprotinin, 5 μg/ml leupeptin, Phosphatase Inhibitor Cocktail 2 (Sigma) at 1:1000). Whole-cell lysates were subjected to analyses by immunoblotting with an Infrared Imaging System (Odyssey; LI-COR Biosciences) as previously described[36]. Antibodies against phospho-Src family (Tyr416) (Cell Signaling, #2101), GFP (Clontech, JL-8), phospho-Erk1/2 (Abcam, ab50011), Erk1/2 (BioSource, 44654G), phospho-Erk5 (Sigma, E7153), Erk5 (Santa Cruz, 12F2), phospho-JNK (Santa Cruz, G-7), JNK (BioSource, 44690), phospho-p38 (Calbiochem, 506124) and p38 (BioSource, 2F11) were purchased commercially.

Immunoprecipitation and in vitro kinase assay

Twenty four hours after transfection of Lyn WT-GFP or Lyn C466A-GFP, HEK293 cells were treated with 5 μM PP2 for 2–4 h to inactivate the basal activity of Lyn. Cells were lysed in cRIPA lysis buffer (50 mM Tris-HCl, pH 7.5, 150 mM NaCl, 1% Triton X-100, 2 mM EGTA, 1mM Na_3VO_4, 1 mM dithiothreitol, 0.2 mM PMSF, 10 μg/ml aprotinin, 5 μg/ml leupeptin, 1 μM PP2, 0.1% SDS, 0.5% sodium deoxycholate). Lyn-GFP was immunoprecipitated with anti-GFP serum (Invitrogen) and GammaBind G-Sepharose beads (GE Healthcare). The immune complex was washed twice with cRIPA buffer (50 mM Tris-HCl, pH 7.5, 150 mM NaCl, 1% Triton X-100, 2 mM EGTA, 0.1% SDS, 0.5% sodium deoxycholate) and twice with kinase buffer (10 mM Tris-HCl, pH7.5, 5 mM $MgCl_2$). The immunoprecipitate was treated with or without 15 μM H_2O_2 in kinase buffer (40 μL) containing 100 μM ATP and 0.5 μg Sam68[37] (Santa Cruz) at room temperature for 45 seconds with continuous mixing[38]. The reaction was stopped by addition of 5x sample buffer and the immunocomplexes were separated by SDS-PAGE and probed with anti-phosphotyrosine antibody (4G10 Platinum, Millipore). The precipitated Lyn and Sam68 were detected by Amido black staining. When we performed the kinase assay to examine effects of magnesium on Lyn activity (Fig. 3g,h), $MgCl_2$ was removed from kinase buffer for washing and the immunoprecipitate was treated with or without 5 mM $MgCl_2$ during the kinase assay.

BIAM-mediated carboxymethylation

Twenty four hours after transfection, HEK293 cells were lysed in cRIPA lysis buffer (50 mM Tris-HCl, pH 7.5, 150 mM NaCl, 1% Triton X-100, 2 mM EGTA, 1mM Na_3VO_4, 0.2 mM PMSF, 10 μg/mlaprotinin, 5 μg/mlleupeptin, 0.1% SDS, 0.5% sodium deoxycholate) containing 100 μM BIAM (Invitrogen). Lyn-GFP was immunoprecipitated with anti-GFP serum (Invitrogen) and GammaBind G-Sepharose beads (GE Healthcare). The immunocomplexes were separated by SDS-PAGE and probed with anti-GFP antibody (JL-8, Clontech) and IRDye 680 Streptavidin (LI-COR Biosciences).

Generation of *Tg(mpx:Lyn-GFP)* and *Tg(mpx:Lyn C466A-GFP)*

One nanoliter of solution containing 12.5 ng/μL DNA plasmid (tol2-mpx-lyn-GFP or tol2-mpx-lyn C466A-GFP) and 17.5 ng/μL transposase mRNA was injected into the cytoplasm of one-cell stage embryos. Injected embryos were raised to sexual maturity and screened by crossing with wild-type fish to identify founders. F1 embryos were identified by GFP expression and raised to sexual maturity. Experiments were performed on progeny of F1 or F2 outcross with wild-type fish.

Purification of human neutrophils and in vitro chemotaxis assay

Blood was obtained from healthy donors with informed consent. Neutrophils were purified using Polymorphprep (Nycomed Pharma AS). Purified neutrophils were suspended in HBSS containing 5% FBS and 25 mM HEPES at 1.5–2.5 × 10^7 cells/ml. Cells were pretreated with DMSO, 10 μM PP2 or 10 μM SU6656 for 30 minutes. The under agarose assay was performed as previously described[39] with minor modification. Plastic tissue culture dishes (35 mm diameter) were filled with 3 ml of a 1.2% agarose solution containing 50% HBSS and 50% RPMI-1640 with 20% FBS. After the agarose solidified, four series of three wells, 2 mm in diameter and spaced 2 mm apart, were made. The center well of each three-well series was loaded with 20 μl of neutrophils (1.5–2.5 × 10^7 cells/ml) and the outer wells were loaded with chemoattractants (10 μM H_2O_2 or 100 nM fMLP) and HBSS. Once loaded, the gels were incubated for 1h in a 37°C/5% CO_2 incubator. Cells were fixed with methanol for a few hours, and with 37% formaldehyde overnight. After fixation, the gels were carefully removed and cells were stained using a Hema-3 stain kit (Thermo Fisher Scientific). For quantification, four dishes were used for each condition. Cells were imaged using a Nikon SMZ-1500 stereomicroscope (Nikon) and acquired pictures were thresholded to generate binary images. Pixel intensities of binary images on each side of the center well were quantified by MetaView software. The pixel intensity on the chemoattraction side was divided by the intensity on the buffer side. The geometric mean of 16 values (Each of four dishes has four series of three wells) was calculated for each condition. The means of three separate experiments were calculated and shown with SEM.

Statistics

All error bars indicate standard errors of means (SEM). For quantification of western blot and in vitro chemotaxis assay, data shown are means ± SEM of at least three separate experiments. For quantification of animal experiments in vivo, representative data of two or

three separate experiments are presented unless otherwise indicated. Assuming Gaussian distribution of overall population of values, P-values were derived by following analyses.

Two-tailed unpaired t-test: Fig. 1c,e,f,i, Fig. 2e,g,i, Fig. 3f,h, Supplementary Fig. 2b,d,e,h, Supplementary Fig. 4g, Supplementary Fig. 7c,e, Supplementary Fig. 11c,f,g

Two-tailed paired t-test: Supplementary Fig. 8c,f, Supplementary Fig. 9c,e

One-way ANOVA with Bonferroni post-test: Fig. 3d, Fig. 4a,c, Supplementary Fig. 4c, f, Supplementary Fig. 7a

One-way ANOVA with Dunnett post-test: Fig. 2d, Fig. 3b, Supplementary Fig. 2f, Supplementary Fig. 5c, Supplementary Fig. 6a, Supplementary Fig. 12a

Supplementary Material

Refer to Web version on PubMed Central for supplementary material.

Acknowledgments

We deeply thank K.T. Chan for help with tissue culture work, J.M. Green, P-Y Lam for help with in situ hybridization, M. Shelef, S. Wernimont for drawing blood, and A.J. Wiemer for insightful discussion and critical reading of the manuscript. This work was supported by American Heart Association fellowship 11PRE4890041 (S.Y.), National Institutes of Health Grants GM074827 (A.H.) and UW Research Training Grant in Hematology 5T32 HL07899 (T.W.S.).

References

1. Nathan C. Neutrophils and immunity: challenges and opportunities. Nat Rev Immunol. 2006; 6:173–182. [PubMed: 16498448]
2. Dvorak HF. Tumors: wounds that do not heal. Similarities between tumor stroma generation and wound healing. N Engl J Med. 1986; 315:1650–1659. [PubMed: 3537791]
3. Klyubin IV, Kirpichnikova KM, Gamaley IA. Hydrogen peroxide-induced chemotaxis of mouse peritoneal neutrophils. Eur J Cell Biol. 1996; 70:347–351. [PubMed: 8864663]
4. Feng Y, Santoriello C, Mione M, Hurlstone A, Martin P. Live imaging of innate immune cell sensing of transformed cells in zebrafish larvae: parallels between tumor initiation and wound inflammation. PLoS Biol. 2010; 8:e1000562. [PubMed: 21179501]
5. Moreira S, Stramer B, Evans I, Wood W, Martin P. Prioritization of competing damage and developmental signals by migrating macrophages in the Drosophila embryo. Curr Biol. 2010; 20:464–470. [PubMed: 20188558]
6. Niethammer P, Grabher C, Look AT, Mitchison TJ. A tissue-scale gradient of hydrogen peroxide mediates rapid wound detection in zebrafish. Nature. 2009; 459:996–999. [PubMed: 19494811]
7. Rhee SG. Cell signaling. H2O2, a necessary evil for cell signaling. Science. 2006; 312:1882–1883. [PubMed: 16809515]
8. Bienert GP, Schjoerring JK, Jahn TP. Membrane transport of hydrogen peroxide. Biochim Biophys Acta. 2006; 1758:994–1003. [PubMed: 16566894]
9. Paulsen CE, Carroll KS. Orchestrating redox signaling networks through regulatory cysteine switches. ACS Chem Biol. 2010; 5:47–62. [PubMed: 19957967]
10. Poole LB, Nelson KJ. Discovering mechanisms of signaling-mediated cysteine oxidation. Curr Opin Chem Biol. 2008; 12:18–24. [PubMed: 18282483]
11. Miller EW, Dickinson BC, Chang CJ. Aquaporin-3 mediates hydrogen peroxide uptake to regulate downstream intracellular signaling. Proc Natl Acad Sci U S A. 2010; 107:15681–15686. [PubMed: 20724658]
12. Burgoyne JR, et al. Cysteine redox sensor in PKGIa enables oxidant-induced activation. Science. 2007; 317:1393–1397. [PubMed: 17717153]

13. Giannoni E, Buricchi F, Raugei G, Ramponi G, Chiarugi P. Intracellular reactive oxygen species activate Src tyrosine kinase during cell adhesion and anchorage-dependent cell growth. Mol Cell Biol. 2005; 25:6391–6403. [PubMed: 16024778]
14. Guo Z, Kozlov S, Lavin MF, Person MD, Paull TT. ATM activation by oxidative stress. Science. 2010; 330:517–521. [PubMed: 20966255]
15. Kemble DJ, Sun G. Direct and specific inactivation of protein tyrosine kinases in the Src and FGFR families by reversible cysteine oxidation. Proc Natl Acad Sci U S A. 2009; 106:5070–5075. [PubMed: 19273857]
16. Mathias JR, et al. Resolution of inflammation by retrograde chemotaxis of neutrophils in transgenic zebrafish. J Leukoc Biol. 2006; 80:1281–1288. [PubMed: 16963624]
17. Tobin DM, et al. The lta4h locus modulates susceptibility to mycobacterial infection in zebrafish and humans. Cell. 2010; 140:717–730. [PubMed: 20211140]
18. Yoo SK, et al. Differential regulation of protrusion and polarity by PI3K during neutrophil motility in live zebrafish. Dev Cell. 2010; 18:226–236. [PubMed: 20159593]
19. Yoo SK, Huttenlocher A. Spatiotemporal photolabeling of neutrophil trafficking during inflammation in live zebrafish. J Leukoc Biol. 2011; 89:661–667. [PubMed: 21248150]
20. Martin GS. The hunting of the Src. Nat Rev Mol Cell Biol. 2001; 2:467–475. [PubMed: 11389470]
21. Sicheri F, Moarefi I, Kuriyan J. Crystal structure of the Src family tyrosine kinase Hck. Nature. 1997; 385:602–609. [PubMed: 9024658]
22. Xu W, Harrison SC, Eck MJ. Three-dimensional structure of the tyrosine kinase c-Src. Nature. 1997; 385:595–602. [PubMed: 9024657]
23. Yeatman TJ. A renaissance for SRC. Nat Rev Cancer. 2004; 4:470–480. [PubMed: 15170449]
24. Scapini P, Pereira S, Zhang H, Lowell CA. Multiple roles of Lyn kinase in myeloid cell signaling and function. Immunol Rev. 2009; 228:23–40. [PubMed: 19290919]
25. Hibbs ML, et al. Multiple defects in the immune system of Lyn-deficient mice, culminating in autoimmune disease. Cell. 1995; 83:301–311. [PubMed: 7585947]
26. Nishizumi H, et al. Impaired proliferation of peripheral B cells and indication of autoimmune disease in lyn-deficient mice. Immunity. 1995; 3:549–560. [PubMed: 7584145]
27. Pereira S, Lowell C. The Lyn tyrosine kinase negatively regulates neutrophil integrin signaling. J Immunol. 2003; 171:1319–1327. [PubMed: 12874221]
28. Lee YM, et al. NOX4 as an oxygen sensor to regulate TASK-1 activity. Cell Signal. 2006; 18:499–507. [PubMed: 16019190]
29. Abe J, Takahashi M, Ishida M, Lee JD, Berk BC. c-Src is required for oxidative stress-mediated activation of big mitogen-activated protein kinase 1. J Biol Chem. 1997; 272:20389–20394. [PubMed: 9252345]
30. Yan SR, Berton G. Regulation of Src family tyrosine kinase activities in adherent human neutrophils. Evidence that reactive oxygen intermediates produced by adherent neutrophils increase the activity of the p58c-fgr and p53/56lyn tyrosine kinases. J Biol Chem. 1996; 271:23464–23471. [PubMed: 8798554]
31. Mathias JR, et al. Characterization of zebrafish larval inflammatory macrophages. Dev Comp Immunol. 2009; 33:1212–1217. [PubMed: 19619578]
32. Bennett CM, et al. Myelopoiesis in the zebrafish, Danio rerio. Blood. 2001; 98:643–651. [PubMed: 11468162]
33. Thisse C, Thisse B. High-resolution in situ hybridization to whole-mount zebrafish embryos. Nat Protoc. 2008; 3:59–69. [PubMed: 18193022]
34. Urasaki A, Morvan G, Kawakami K. Functional dissection of the Tol2 transposable element identified the minimal cis-sequence and a highly repetitive sequence in the subterminal region essential for transposition. Genetics. 2006; 174:639–649. [PubMed: 16959904]
35. Belousov VV, et al. Genetically encoded fluorescent indicator for intracellular hydrogen peroxide. Nat Methods. 2006; 3:281–286. [PubMed: 16554833]
36. Chan KT, Cortesio CL, Huttenlocher A. FAK alters invadopodia and focal adhesion composition and dynamics to regulate breast cancer invasion. J Cell Biol. 2009; 185:357–370. [PubMed: 19364917]

37. Wong BR, et al. TRANCE, a TNF family member, activates Akt/PKB through a signaling complex involving TRAF6 and c-Src. Mol Cell. 1999; 4:1041–1049. [PubMed: 10635328]

38. Yamanashi Y, et al. Activation of Src-like protein-tyrosine kinase Lyn and its association with phosphatidylinositol 3-kinase upon B-cell antigen receptor-mediated signaling. Proc Natl Acad Sci U S A. 1992; 89:1118–1122. [PubMed: 1371009]

39. Heit B, Kubes P. Measuring chemotaxis and chemokinesis: the under-agarose cell migration assay. Sci STKE. 2003:PL5. [PubMed: 12591998]

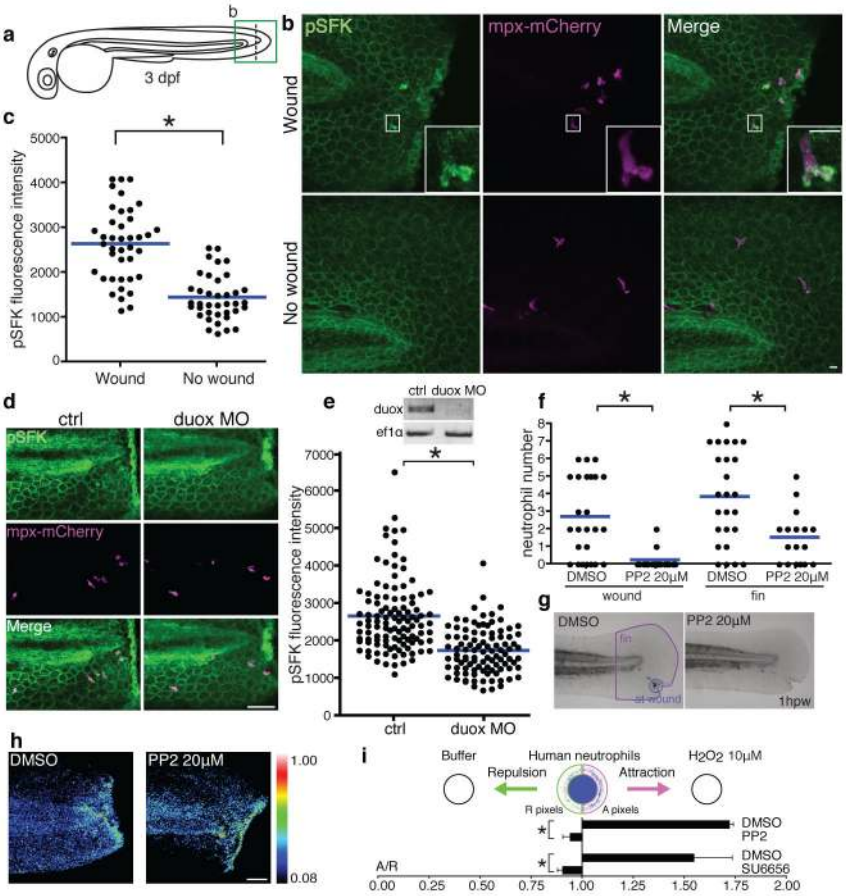

Figure 1. SFKs mediate neutrophil wound response

a, Diagram of tail-transection in 3 dpf zebrafish larvae. **b,** Immunofluorescence of pSFK (phosphorylation of SFK activation loop tyrosine) in *Tg(mpx:mCherry)*. mCherry labels neutrophils. **c,** Quantification of fluorescence intensity of pSFK in neutrophils (wound: 40 cells (5 larvae), no wound: 38 cells (7 larvae)). **d,** Immunofluorescence of pSFK in *Tg(mpx:mCherry)* with/without duox morpholino. **e,** RT-PCR of duox mRNA with/without duox morpholino (ef1α is a loading control) and quantification of fluorescence intensity of pSFK in neutrophils (ctrl: 110 cells (13 larvae), duox MO: 98 cells (19 larvae). **f,** Neutrophil recruitment to wounds and fins at 1h post wounding with/without PP2 (DMSO: 25 larvae, PP2: 17 larvae). **g,** Representative pictures of Sudan Black staining. **h,** H_2O_2 imaging with HyPer probe with/without PP2. **i,** Under-agarose assay using human neutrophils (n=3). Error bars indicate SEM. Asterisk, P<0.05, two-tailed unpaired t-test (c,e,f,i). Scale bars: 10 μm (b), 50 μm (d,h)

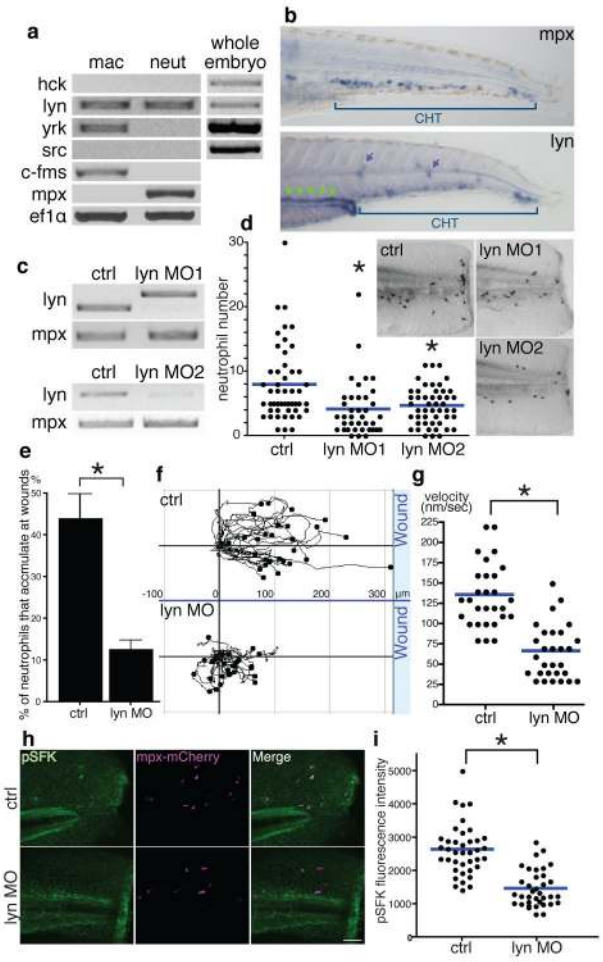

Figure 2. Lyn mediates neutrophil wound responses

a, RT-PCR of SFKs. c-fms and mpx are markers of macrophages and neutrophils respectively and ef1α is a loading control. **b,** In situ hybridization of mpx and lyn mRNA. Green arrowheads: pronephric ducts, purple arrows: neuromasts. **c,** RT-PCR of lyn with/without lyn morpholinos. **d,** Neutrophil wound recruitment with/without lyn morpholinos at 30 minutes post wounding (ctrl: 49 larvae, lyn MO1: 38 larvae, lyn MO2: 50 larvae). Pictures display Sudan Black staining. **e,** The percentage of neutrophils that accumulate at wounds during 30 minutes post wounding (14 larvae each). **f,** Neutrophil tracking for 25 minutes post wounding (29 cells, 6 larvae each). **g,** Neutrophil velocity during wound responses (29 cells, 6 larvae each). **h,** Immunofluorescence of pSFK in *Tg(mpx:mCherry)* with/without lyn morpholino. **i,** Quantification of fluorescence intensity of pSFK in neutrophils (ctrl: 39 cells (4 larvae), lyn MO: 36 cells (5 larvae)). Error bars indicate SEM. Asterisk, $P<0.05$, one-way ANOVA with Dunnett post-test (d) and two-tailed unpaired t-test (e,g,i). Scale bar: 50 μm.

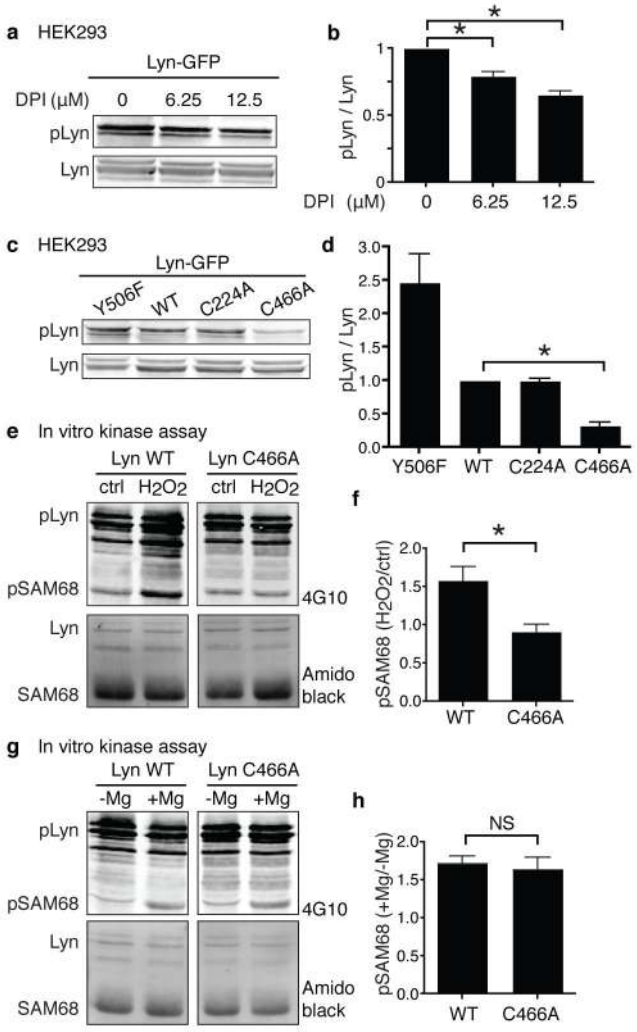

Figure 3. H_2O_2 activates Lyn in a C466-dependent manner

a, Autophosphorylation of Lyn activation loop tyrosine with/without DPI in HEK293 cells. **b,** Quantification of a (n=4). **c,** Autophosphorylation of Lyn mutants in HEK 293 cells. Y506F is a constitutively active mutant as a positive control of pLyn. **d,** Quantification of c (n=3). **e,** In vitro kinase assay of Lyn WT and C466A with/without H_2O_2. **f,** Quantification of e (n=6). **g,** In vitro kinase assay of Lyn WT and C466A with/without magnesium. **h,** Quantification of g (n=5). Error bars indicate SEM. Asterisk, P<0.05, one-way ANOVA with Dunnett post test (b), Bonferroni post-test (d) and two-tailed unpaired t-test (f,h).

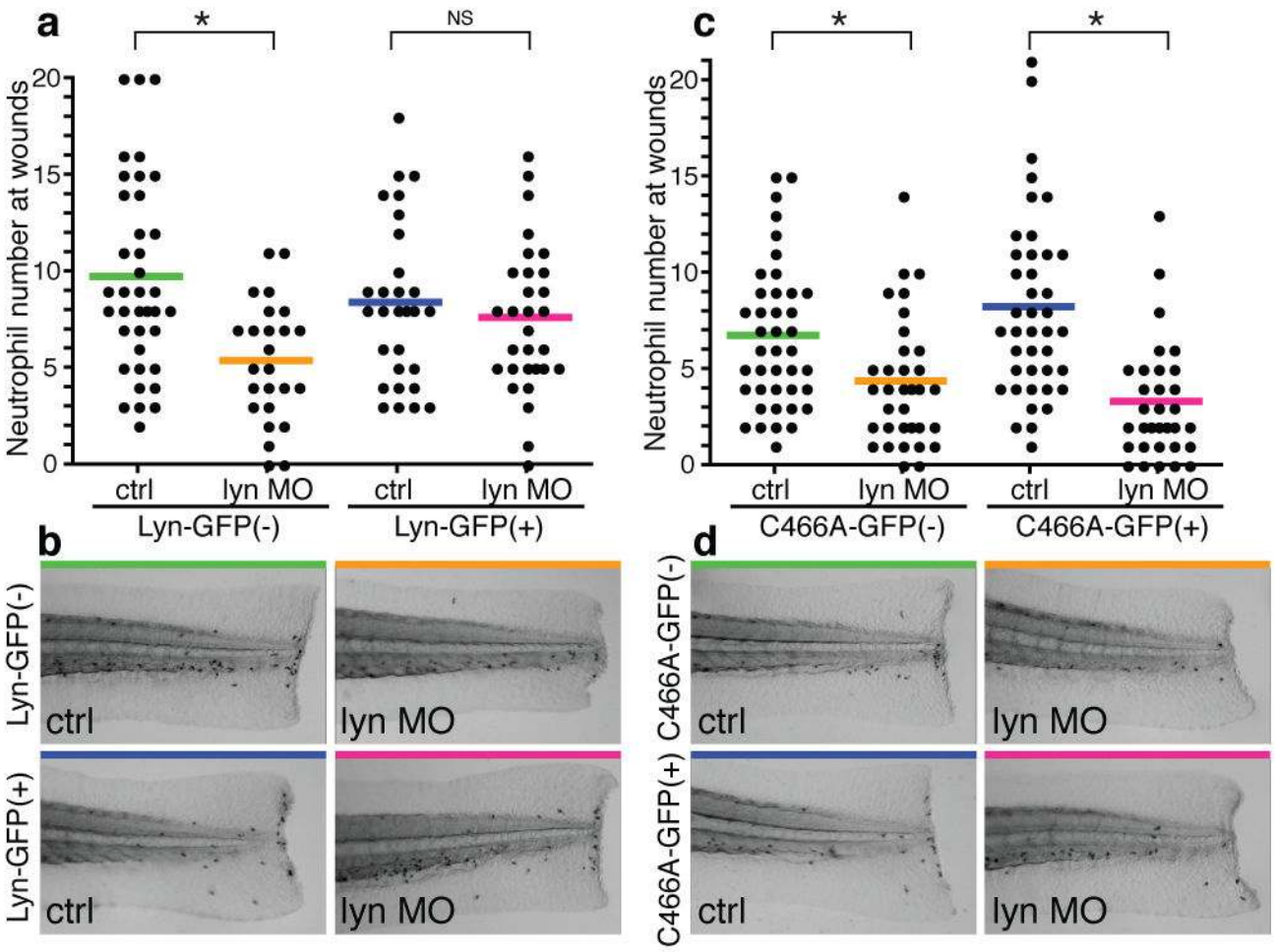

Figure 4. Lyn regulates neutrophil wound responses in a C466-dependent manner

a, Neutrophil wound recruitment with/without lyn morpholino in *Tg(mpx:lyn-GFP)* and wild-type clutchmates (Lyn-GFP(−)/ctrl: 38 larvae, Lyn-GFP(−)/lyn MO: 29 larvae, Lyn-GFP(+)/ctrl: 26 larvae, Lyn-GFP(+)/lyn MO: 30 larvae). **b,** Representative pictures of Sudan Black staining in a. **c,** Neutrophil wound recruitment with/without lyn morpholino in *Tg(mpx:lyn C466A-GFP)* and wild-type clutchmates (C466A-GFP(−)/ctrl: 41 larvae, C466A-GFP(−)/lyn MO: 41larvae, C466A-GFP(+)/ctrl: 34 larvae, C466A-GFP(+)/lyn MO: 32 larvae). **d,** Representative pictures of Sudan Black staining in c. Asterisk, $P<0.05$, one-way ANOVA with Bonferroni post-test (a,c).